COMMUNICATIONS IN COMPUTATIONAL PHYSICS
Vol. **4**, No. 1, pp. 135-160

Commun. Comput. Phys.
July 2008

A Uniformly Convergent Numerical Method for Singularly Perturbed Nonlinear Eigenvalue Problems

Weizhu Bao[1,*] and Ming-Huang Chai[2,3]

[1] *Department of Mathematics and Center for Computational Science and Engineering, National University of Singapore, 117543, Singapore.*
[2] *Department of Mathematics, National University of Singapore, 117543, Singapore.*
[3] *NUS High School, National University of Singapore, 117543, Singapore.*

Received 22 August 2007; Accepted (in revised version) 15 October 2007

Available online 27 February 2008

Abstract. In this paper we propose a uniformly convergent numerical method for discretizing singularly perturbed nonlinear eigenvalue problems under constraints with applications in Bose-Einstein condensation and quantum chemistry. We begin with the time-independent Gross-Pitaevskii equation and show how to reformulate it into a singularly perturbed nonlinear eigenvalue problem under a constraint. Matched asymptotic approximations for the problem are presented to locate the positions and characterize the widths of boundary layers and/or interior layers in the solution. A uniformly convergent numerical method is proposed by using the normalized gradient flow and piecewise uniform mesh techniques based on the asymptotic approximations for the problem. Extensive numerical results are reported to demonstrate the effectiveness of our numerical method for the problems. Finally, the method is applied to compute ground and excited states of Bose-Einstein condensation in the semiclassical regime and some conclusive findings are reported.

AMS subject classifications: 35P30, 35Q55, 65N25, 65N06, 81Q05, 81V45

Key words: Nonlinear eigenvalue problem, Bose-Einstein condensation, ground state, excited state, energy, chemical potential, piecewise uniform mesh.

1 Introduction

We consider the following nonlinear eigenvalue problem [2, 5, 10]

$$\mu\phi(\mathbf{x}) = -\frac{1}{2}\nabla^2\phi(\mathbf{x}) + V(\mathbf{x})\phi(\mathbf{x}) + \beta|\phi(\mathbf{x})|^2\phi(\mathbf{x}), \qquad \mathbf{x}\in\Omega\subset\mathbb{R}^d, \tag{1.1}$$

$$\phi(\mathbf{x}) = 0, \qquad \mathbf{x}\in\partial\Omega, \tag{1.2}$$

*Corresponding author. *Email addresses:* bao@math.nus.edu.sg (W. Z. Bao), nhscmh@nus.edu.sg (M. H. Chai)

where $\mathbf{x}=(x_1,\cdots,x_d)^T$ is the spatial coordinate, Ω is a subdomain of $\mathbb{R}^d$ ($d=1,2,3$), $V(\mathbf{x})$ is a real-valued potential whose shape is determined by the type of system under investigation, and β is a constant. Eq. (1.1) is also known as the time-independent Gross-Pitaevskii equation (GPE) in Bose-Einstein condensation (BEC) [3, 7, 24], where ϕ is the macroscopic wave function of the condensate and β positive/negative corresponds to repulsive/attractive interaction between atoms. The wave function ϕ is required to satisfy the normalization condition

$$\|\phi\|^2 := \int_\Omega |\phi(\mathbf{x})|^2 \, d\mathbf{x} = 1. \tag{1.3}$$

For the nonlinear eigenvalue problem (1.1)-(1.2) under the constraint (1.3), any eigenvalue μ which is also called as chemical potential in quantum physics can be computed from its corresponding eigenfunction ϕ by

$$\begin{aligned}\mu := \mu_\beta(\phi) &= \int_\Omega \left[\frac{1}{2}|\nabla\phi(\mathbf{x})|^2 + V(\mathbf{x})|\phi(\mathbf{x})|^2 + \beta|\phi(\mathbf{x})|^4\right] d\mathbf{x} \\ &= E_\beta(\phi) + \frac{\beta}{2}\int_\Omega |\phi(\mathbf{x})|^4 \, d\mathbf{x},\end{aligned} \tag{1.4}$$

where $E_\beta(\phi)$ is the energy per particle in BEC and is defined as

$$E_\beta(\phi) = \int_\Omega \left[\frac{1}{2}|\nabla\phi(\mathbf{x})|^2 + V(\mathbf{x})|\phi(\mathbf{x})|^2 + \frac{\beta}{2}|\phi(\mathbf{x})|^4\right] d\mathbf{x}. \tag{1.5}$$

In fact, the nonlinear eigenvalue problem (1.1)-(1.2) can be viewed as the Euler-Lagrange equation of the energy functional $E_\beta(\phi)$ in (1.5) under the constraint (1.3). In physics literatures [3, 7, 24], the ground state is defined as the minimizer of the energy functional in (1.5) over the unit sphere

$$S = \{\phi \mid \|\phi\| = 1, \quad E_\beta(\phi) < \infty\}.$$

Any other eigenfunctions of the nonlinear eigenvalue problem (1.1)-(1.2) under the constraint (1.3), whose energy are greater than that of the ground state, are usually known as excited states.

Different numerical methods were proposed in the literatures for computing the eigenfunctions, i.e., ground and excited states, of the nonlinear eigenvalue problem (1.1)-(1.2) under the constraint (1.3). For example, Edwards and Burnett [21] presented a Runge-Kutta type method and used it to solve one dimensional (1D) and 3D ground states with spherical symmetry. Adhikari [1] used this approach to get the ground state solution of GPE in 2D with radial symmetry. Ruprecht et al. [26] used the Crank-Nicolson finite difference method for solving BEC ground state. Bao and Tang [10] proposed a method by directly minimizing the energy functional via finite element approximation to obtain the ground and excited states. Bao and Du [5] presented a continuous normalized gradient

flow with diminishing energy and discretized it with a backward Euler finite difference (BEFD) and time-splitting sine-pseudospectral method (TSSP) for computing the ground and first excited states in BEC. This idea was extended to multi-component BEC [4, 6], rotating BEC [12] and spin-1 BEC [8, 11]. Chang et al. [16, 17] proposed Gauss-Seidel-type methods for computing positive bound states of a multi-component BEC. Chang et al. [15] presented the Liapunov-Schmidt reduction and continuation method for computing ground states of single- and multi-component BEC. Zhou [33, 34] and Shen and Zhou [28] provided error estimates for the finite element approximations for some nonlinear eigenvalue problems. Other approaches include an explicit imaginary-time algorithm used by Cerimele et al. [13] and Chiofalo et al. [18], a direct inversion in the iterated subspace (DIIS) used by Schneider et al. [27], and a simple analytical type method proposed by Dodd [20]. As observed in [9], when $\beta \gg 1$, boundary and/or interior layers appear in the ground and excited states when $V(\mathbf{x})$ is chosen as a box potential, and interior layers appear in the excited states when $V(\mathbf{x})$ is chosen as the harmonic potential. In these cases, all the above numerical methods which in general use uniform meshes do not converge uniformly with respect to $\beta \gg 1$. The aim of this paper is to propose a uniformly convergent numerical method for the nonlinear eigenvalue problem (1.1)-(1.2) under the constraint (1.3) based on the normalized gradient flow proposed for computing ground state of BEC [4, 5, 12] and piecewise uniform mesh techniques used for singularly perturbed two-point boundary value problems [22, 23, 25, 29–32].

The paper is organized as follows. In Section 2, we reformulate the time-independent GPE (1.1) into a singularly perturbed nonlinear eigenvalue problem when $\beta \gg 1$. In Section 3, we present matched asymptotic approximations of the eigenfunctions and chemical potential as well as energy. In Section 4, we propose a uniformly convergent numerical method by using the normalized gradient flow and piecewise uniform mesh techniques for discretizing the singularly perturbed nonlinear eigenvalue problem under a constraint. In Section 5, extensive numerical results are reported to demonstrate the efficiency of our numerical method and to compare with other existing numerical methods. Finally, some conclusions are drawn in Section 6.

2 A singularly perturbed nonlinear eigenvalue problem

In this section, we reformulate the time-independent GPE (1.1) with either box potential or harmonic potential into a singularly perturbed nonlinear eigenvalue problem under a constraint when $\beta \gg 1$, i.e., it is in strongly repulsive interaction regime.

2.1 For bounded Ω with the box potential

When Ω is bounded and $V(\mathbf{x})$ is chosen as the box potential, i.e., $V(\mathbf{x}) \equiv 0$ when $\mathbf{x} \in \Omega$ and $V(\mathbf{x}) = \infty$ otherwise, let

$$\varepsilon := \frac{1}{\sqrt{\beta}}, \qquad \mu^\varepsilon := \varepsilon^2 \mu = \frac{\mu}{\beta}, \qquad \phi^\varepsilon(\mathbf{x}) = \phi(\mathbf{x}). \tag{2.1}$$

Divided by β at both sides of (1.1), the time-independent GPE (1.1)-(1.2) under the constraint (1.3) is reformulated to the following singularly perturbed nonlinear eigenvalue problem

$$\mu^\varepsilon \phi^\varepsilon(\mathbf{x}) = -\frac{\varepsilon^2}{2}\nabla^2\phi^\varepsilon(\mathbf{x}) + |\phi^\varepsilon(\mathbf{x})|^2\phi^\varepsilon(\mathbf{x}), \qquad \mathbf{x}\in\Omega, \tag{2.2}$$

$$\phi^\varepsilon(\mathbf{x}) = 0, \qquad \mathbf{x}\in\partial\Omega; \tag{2.3}$$

under the constraint

$$\|\phi^\varepsilon\|^2 := \int_\Omega |\phi^\varepsilon(\mathbf{x})|^2\, d\mathbf{x} = 1. \tag{2.4}$$

The eigenvalue (or chemical potential) μ^ε can be computed from its corresponding eigenfunction ϕ^ε by

$$\begin{aligned}\mu^\varepsilon &:= \mu_\varepsilon(\phi^\varepsilon) = \int_\Omega \left[\frac{\varepsilon^2}{2}|\nabla\phi^\varepsilon(\mathbf{x})|^2 + |\phi^\varepsilon(\mathbf{x})|^4\right] d\mathbf{x} \\ &= E_\varepsilon(\phi^\varepsilon) + \frac{1}{2}\int_\Omega |\phi^\varepsilon(\mathbf{x})|^4\, d\mathbf{x},\end{aligned} \tag{2.5}$$

where the re-scaled energy $E_\varepsilon(\phi^\varepsilon)$ is defined as

$$E_\varepsilon(\phi^\varepsilon) = \int_\Omega \left[\frac{\varepsilon^2}{2}|\nabla\phi^\varepsilon(\mathbf{x})|^2 + \frac{1}{2}|\phi^\varepsilon(\mathbf{x})|^4\right] d\mathbf{x}. \tag{2.6}$$

By assuming that ϕ^ε is ε-oscillatory (i.e., $\phi^\varepsilon(\mathbf{x}) = \sqrt{\rho^\varepsilon(\mathbf{x})}\, e^{iS^\varepsilon(\mathbf{x})/\varepsilon}$ with $\rho^\varepsilon(\mathbf{x}) = |\phi^\varepsilon(\mathbf{x})|^2$ and $S^\varepsilon(\mathbf{x}) = \varepsilon\arg(\phi^\varepsilon(\mathbf{x}))$, the position density and phase of the wave function ϕ^ε, respectively) and sufficiently 'integrable' such that all terms have $\mathcal{O}(1)$-integral in (2.5) and (2.6) and noting (2.4), we have [7, 9]

$$\mu^\varepsilon = \mu_\varepsilon(\phi^\varepsilon) = \mathcal{O}(1), \qquad E_\varepsilon(\phi^\varepsilon) = \mathcal{O}(1), \qquad 0 < \varepsilon \ll 1. \tag{2.7}$$

Then the leading asymptotic approximations of the eigenvalue in (1.4) and energy in (1.5) in this case can be given by

$$\mu = \mu_\beta(\phi) = \beta\int_\Omega \left[\frac{1}{2\beta}|\nabla\phi(\mathbf{x})|^2 + |\phi(\mathbf{x})|^4\right] d\mathbf{x} = \beta\,\mu_\varepsilon(\phi^\varepsilon) = \mathcal{O}(\beta), \tag{2.8}$$

$$E_\beta(\phi) = \beta\int_\Omega \left[\frac{1}{2\beta}|\nabla\phi(\mathbf{x})|^2 + \frac{1}{2}|\phi(\mathbf{x})|^4\right] d\mathbf{x} = \beta\, E_\varepsilon(\phi^\varepsilon) = \mathcal{O}(\beta), \quad \beta \gg 1. \tag{2.9}$$

2.2 For the whole space $\Omega = \mathbb{R}^d$ with the harmonic potential

When $\Omega = \mathbb{R}^d$ is the whole space and $V(\mathbf{x})$ is chosen as the harmonic potential, i.e.,

$$V(\mathbf{x}) = \frac{1}{2}\left(\gamma_1^2 x_1^2 + \cdots + \gamma_d^2 x_d^2\right)$$

with $\gamma_1,\cdots,\gamma_d$ positive constants, under the normalization (1.3), we choose the semiclassical re-scaling as

$$\mathbf{x}=\varepsilon^{1/2}\tilde{\mathbf{x}},\quad \phi^\varepsilon(\tilde{\mathbf{x}})=\varepsilon^{-d/4}\phi(\mathbf{x}),\quad \mu^\varepsilon=\varepsilon^{-1}\mu,\quad \text{with}\quad \varepsilon=\beta^{-d/(d+2)}. \tag{2.10}$$

Substituting the above re-scaling parameters into (1.1), rearranging the parameters and dropping the $\tilde{}$, we again obtain a singularly perturbed nonlinear eigenvalue problem

$$\mu^\varepsilon\phi^\varepsilon(\mathbf{x})=-\frac{\varepsilon^2}{2}\nabla^2\phi^\varepsilon(\mathbf{x})+V(\mathbf{x})\phi^\varepsilon(\mathbf{x})+|\phi^\varepsilon(\mathbf{x})|^2\phi^\varepsilon(\mathbf{x}),\qquad \mathbf{x}\in\mathbb{R}^d, \tag{2.11}$$

under the constraint

$$\|\phi^\varepsilon\|^2:=\int_{\mathbb{R}^d}|\phi^\varepsilon(\mathbf{x})|^2\,d\mathbf{x}=1. \tag{2.12}$$

Again, the eigenvalue (or chemical potential) μ^ε can be computed from its corresponding eigenfunction ϕ^ε by

$$\begin{aligned}\mu^\varepsilon &:= \mu_\varepsilon(\phi^\varepsilon)=\int_{\mathbb{R}^d}\left[\frac{\varepsilon^2}{2}|\nabla\phi^\varepsilon(\mathbf{x})|^2+V(\mathbf{x})|\phi^\varepsilon(\mathbf{x})|^2+|\phi^\varepsilon(\mathbf{x})|^4\right]d\mathbf{x}\\ &= E_\varepsilon(\phi^\varepsilon)+\frac{1}{2}\int_{\mathbb{R}^d}|\phi^\varepsilon(\mathbf{x})|^4\,d\mathbf{x},\end{aligned} \tag{2.13}$$

where the re-scaled energy $E_\varepsilon(\phi^\varepsilon)$ is defined as

$$E_\varepsilon(\phi^\varepsilon)=\int_{\mathbb{R}^d}\left[\frac{\varepsilon^2}{2}|\nabla\phi^\varepsilon(\mathbf{x})|^2+V(\mathbf{x})|\phi^\varepsilon(\mathbf{x})|^2+\frac{1}{2}|\phi^\varepsilon(\mathbf{x})|^4\right]d\mathbf{x}. \tag{2.14}$$

Again, by assuming that ϕ^ε is ε-oscillatory and sufficiently 'integrable' such that all terms have $\mathcal{O}(1)$-integral in (2.13) and (2.14) and noting (2.12), we have

$$\mu^\varepsilon=\mu_\varepsilon(\phi^\varepsilon)=\mathcal{O}(1),\qquad E_\varepsilon(\phi^\varepsilon)=\mathcal{O}(1),\qquad 0<\varepsilon\ll 1. \tag{2.15}$$

Then the leading asymptotic approximations of the eigenvalue in (1.4) and energy in (1.5) in this case can be given by

$$\mu=\mu_\beta(\phi)=\varepsilon^{-1}\mu_\varepsilon(\phi^\varepsilon)=\mathcal{O}(\varepsilon^{-1})=\mathcal{O}(\beta^{d/(d+2)}), \tag{2.16}$$

$$E_\beta(\phi)=\varepsilon^{-1}E_\varepsilon(\phi^\varepsilon)=\mathcal{O}(\varepsilon^{-1})=\mathcal{O}(\beta^{d/(d+2)}),\qquad \beta\gg 1. \tag{2.17}$$

2.3 General formulation

Thus in this paper, we will consider the following singularly perturbed nonlinear eigenvalue problem

$$\mu^\varepsilon\phi^\varepsilon(\mathbf{x})=-\frac{\varepsilon^2}{2}\nabla^2\phi^\varepsilon(\mathbf{x})+V(\mathbf{x})\phi^\varepsilon(\mathbf{x})+|\phi^\varepsilon(\mathbf{x})|^2\phi^\varepsilon(\mathbf{x}),\quad \mathbf{x}\in\Omega\subset\mathbb{R}^d, \tag{2.18}$$

$$\phi^\varepsilon(\mathbf{x})=0,\qquad \mathbf{x}\in\partial\Omega, \tag{2.19}$$

under the normalization or constraint

$$\|\phi^\varepsilon\|^2 := \int_\Omega |\phi^\varepsilon(\mathbf{x})|^2 \, d\mathbf{x} = 1, \tag{2.20}$$

where $0 < \varepsilon \ll 1$ is constant, $V(\mathbf{x})$ is a given real-valued potential.

The eigenvalue (or chemical potential) μ^ε can be computed from its corresponding eigenfunction ϕ^ε by

$$\begin{aligned} \mu^\varepsilon &:= \mu_\varepsilon(\phi^\varepsilon) = \int_\Omega \left[\frac{\varepsilon^2}{2} |\nabla \phi^\varepsilon(\mathbf{x})|^2 + V(\mathbf{x}) |\phi^\varepsilon(\mathbf{x})|^2 + |\phi^\varepsilon(\mathbf{x})|^4 \right] d\mathbf{x} \\ &= E_\varepsilon(\phi^\varepsilon) + \frac{1}{2} \int_\Omega |\phi^\varepsilon(\mathbf{x})|^4 \, d\mathbf{x}, \end{aligned} \tag{2.21}$$

and the energy functional is defined as

$$E_\varepsilon(\phi^\varepsilon) = \int_\Omega \left[\frac{\varepsilon^2}{2} |\nabla \phi^\varepsilon(\mathbf{x})|^2 + V(\mathbf{x}) |\phi^\varepsilon(\mathbf{x})|^2 + \frac{1}{2} |\phi^\varepsilon(\mathbf{x})|^4 \right] d\mathbf{x}. \tag{2.22}$$

Again, the ground state wave function $\phi_g^\varepsilon := \phi_g^\varepsilon(\mathbf{x})$ of a BEC is found by minimizing the energy functional $E_\varepsilon(\phi^\varepsilon)$ over the unit sphere

$$S = \{\phi^\varepsilon(\mathbf{x}) \mid \|\phi^\varepsilon\| = 1, \, E_\varepsilon(\phi^\varepsilon) < \infty\},$$

i.e., find $(\mu_g^\varepsilon, \phi_g^\varepsilon)$ such that

$$E_g^\varepsilon := E_\varepsilon(\phi_g^\varepsilon) = \min_{\phi^\varepsilon \in S} E_\varepsilon(\phi^\varepsilon), \qquad \mu_g^\varepsilon = \mu_\beta^\varepsilon(\phi_g^\varepsilon).$$

It can be easily shown that the ground state $\phi_g^\varepsilon(\mathbf{x})$ is an eigenfunction of the nonlinear eigenvalue problem (2.18) under the constraint (2.20). Any other eigenfunction $\phi^\varepsilon(\mathbf{x})$ of (2.18) under the constraint (2.20) whose energy $E_\varepsilon(\phi^\varepsilon) > E_\varepsilon(\phi_g^\varepsilon)$ is usually known as an excited state in physics literatures. In addition, suppose all different eigenfunctions of the singularly perturbed nonlinear eigenvalue problem (2.18)-(2.19) under the constraint (2.20) are

$$\phi_g^\varepsilon(\mathbf{x}), \quad \phi_1^\varepsilon(\mathbf{x}), \quad \phi_2^\varepsilon(\mathbf{x}), \quad \cdots, \tag{2.23}$$

which are ranked according to their energies, i.e.,

$$E_\varepsilon(\phi_g^\varepsilon) < E_\varepsilon(\phi_1^\varepsilon) < E_\varepsilon(\phi_2^\varepsilon) < \cdots, \tag{2.24}$$

then $\phi_j^\varepsilon(\mathbf{x})$ $(j = 1,2,\cdots)$ is usually known as the j-th excited state in quantum physics.

3 Matched asymptotic approximations

In this section we will present matched asymptotic approximations for the ground state and excited states as well as their energy and chemical potential of the singularly perturbed nonlinear eigenvalue problems (2.18)-(2.19) under the constraint (2.20). We want to mention that similar results for (1.1)-(1.2) with $\beta \gg 1$ were presented in [9].

3.1 For bounded Ω with box potential

For simplicity, here we only present results for $d=1$ and $\Omega=(0,1)$ with the box potential, i.e., $V(x)=0$ for $0\le x\le 1$ and $V(x)=\infty$ otherwise. Extensions to d-dimensions with $\Omega=(0,1)^d$ are straightforward. In this case, when $0<\varepsilon\ll 1$, we formally drop the first term on the right hand side of (2.2) with $\Omega=(0,1)$ and obtain the Thomas-Fermi approximation of the ground state as

$$\mu_g^{\rm TF}\phi_g^{\rm TF}(x)=|\phi_g^{\rm TF}(x)|^2\phi_g^{\rm TF}(x),\qquad 0<x<1, \tag{3.1}$$

which implies

$$\phi_g^{\rm TF}(x)=\sqrt{\mu_g^{\rm TF}},\qquad 0<x<1. \tag{3.2}$$

Plugging (3.2) into the constraint (2.4) with $\Omega=(0,1)$, we get

$$1=\int_0^1|\phi_g^{\rm TF}(x)|^2\,dx=\int_0^1\mu_g^{\rm TF}\,dx=\mu_g^{\rm TF}. \tag{3.3}$$

Here the leading order approximation for the ground state is given by

$$\phi_g^{\varepsilon}(x)\approx\phi_g^{\rm TF}(x)=1,\qquad 0<x<1. \tag{3.4}$$

However, the approximation for the ground state (3.4) does *not* satisfy the zero boundary condition (2.3). This suggests the existence of two boundary layers in the region near $x=0$ and $x=1$ in the ground state of BEC with the box potential.

To get the matched asymptotic approximation, since the two boundary layers exist at the two boundaries $x=0$ and $x=1$ when $0<\varepsilon\ll 1$, we solve (2.2) with $\Omega=(0,1)$ near $x=0$ and $x=1$, respectively. Let us assume that the boundary layer is of width δ with $0<\delta\ll 1$ and do a rescaling in the region near $x=0$ with

$$x=\delta X,\qquad \phi^{\varepsilon}(x)=\phi_s\Phi(X),\qquad X\ge 0. \tag{3.5}$$

Substituting (3.5) into (2.2) with $\Omega=(0,1)$, we obtain

$$\mu^{\varepsilon}\Phi(X)=-\frac{\varepsilon^2}{2\delta^2}\Phi_{XX}(X)+\phi_s^2\Phi(X),\qquad X>0, \tag{3.6}$$

$$\Phi(0)=0,\qquad \lim_{X\to\infty}\Phi(X)=1. \tag{3.7}$$

In order to balance all the terms in (2.2), we need to choose

$$\delta=\frac{\varepsilon}{\sqrt{\mu^{\varepsilon}}},\qquad \phi_s=\sqrt{\mu^{\varepsilon}}. \tag{3.8}$$

Solving the problem (3.6)-(3.7) with the choice of the parameters in (3.8), we get

$$\Phi(X)=\tanh(X),\qquad X\ge 0. \tag{3.9}$$

Since $\mu^\varepsilon \approx \mu_g^{\rm TF} = 1$ for the ground state, we can conclude that the width of the boundary layer near $x=0$ is $\delta = \mathcal{O}(\varepsilon) = \mathcal{O}(\beta^{-1/2})$ and the inner expansion for (2.2)-(2.3) near $x=0$ is

$$\phi_g^\varepsilon(x) \approx \sqrt{\mu_g^\varepsilon}\tanh\left(\sqrt{\mu_g^\varepsilon}x/\varepsilon\right), \qquad \text{for} \quad x \geq 0 \quad \text{near} \quad x=0. \tag{3.10}$$

Similarly, we can get the inner expansion for (2.2)-(2.3) near $x=1$ as

$$\phi_g^\varepsilon(x) \approx \sqrt{\mu_g^\varepsilon}\tanh\left(\sqrt{\mu_g^\varepsilon}(1-x)/\varepsilon\right), \qquad \text{for} \quad x \leq 1 \quad \text{near} \quad x=1. \tag{3.11}$$

Using the matched asymptotic technique, we get the asymptotic approximation for the ground state as

$$\begin{aligned}\phi_g^\varepsilon(x) \approx \phi_g^{\rm MA}(x) \;=\; & \sqrt{\mu_g^{\rm MA}}\left[\tanh\left(\sqrt{\mu_g^{\rm MA}}x/\varepsilon\right)+\tanh\left(\sqrt{\mu_g^{\rm MA}}(1-x)/\varepsilon\right)\right. \\ & \left.-\tanh\left(\sqrt{\mu_g^{\rm MA}}/\varepsilon\right)\right], \qquad 0 \leq x \leq 1.\end{aligned} \tag{3.12}$$

Plugging (3.12) into the normalization constraint (2.4) with $\Omega=(0,1)$, after some computations [9], we obtain

$$1 = \int_0^1 |\phi_g^{\rm MA}(x)|^2\,dx \approx \mu_g^{\rm MA} - 2\varepsilon\sqrt{\mu_g^{\rm MA}}. \tag{3.13}$$

Solving the above equation, we obtain the asymptotic approximation for the chemical potential of the ground state as

$$\mu_g^\varepsilon \approx \mu_g^{\rm MA} = 1 + 2\varepsilon\sqrt{1+\varepsilon^2} + 2\varepsilon^2, \qquad 0 < \varepsilon \ll 1. \tag{3.14}$$

Moreover, plugging (3.12) into (2.6) with $\Omega=(0,1)$, after some computations [9], we obtain the asymptotic approximation for the energy of the ground state as

$$\begin{aligned}E_g^\varepsilon \;\approx\; & E_g^{\rm MA} \approx \frac{1}{2}\mu_g^{\rm MA} + \frac{1}{3}\mu_g^{\rm MA}\varepsilon\sqrt{\mu_g^{\rm MA}} \\ \approx\; & \frac{1}{2} + \frac{4}{3}\varepsilon\sqrt{1+\varepsilon^2} + 2\varepsilon^2, \qquad 0 < \varepsilon \ll 1.\end{aligned} \tag{3.15}$$

Similarly, for the kth ($k \in \mathbb{N}$) excited state of (2.2)-(2.4) with $\Omega=(0,1)$ when $0<\varepsilon\ll 1$, there are two boundary layers near $x=0$ and $x=1$ and k interior layers located at $x_j = \frac{j}{k+1}$ ($j=1,2,\cdots,k$). By using the matched asymptotic technique, we get the asymptotic approximation for the kth excited state as [9]

$$\begin{aligned}\phi_k^\varepsilon(x) \;\approx\; & \phi_k^{\rm MA}(x) = \sqrt{\mu_k^{\rm MA}}\left[\sum_{j=0}^{[(k+1)/2]}\tanh\left(\frac{\sqrt{\mu_k^{\rm MA}}}{\varepsilon}\left(x-\frac{2j}{k+1}\right)\right)\right. \\ & \left.+\sum_{j=0}^{[k/2]}\tanh\left(\frac{\sqrt{\mu_k^{\rm MA}}}{\varepsilon}\left(\frac{2j+1}{k+1}-x\right)\right)-C_k\tanh\left(\frac{\sqrt{\mu_k^{\rm MA}}}{\varepsilon}\right)\right],\end{aligned} \tag{3.16}$$

where $[\tau]$ takes the integer part of the real number τ, the constant $C_k=1$ when k is odd and $C_k=0$ when k is even, and $\mu_k^{\rm MA}$ is the asymptotic approximation of eigenvalue (or chemical potential) of the kth ($k\in\mathbb{N}$) excited state given as [9]

$$\begin{aligned}\mu_k &:= \mu_\varepsilon(\phi_k^\varepsilon)\approx\mu_k^{\rm MA}\\ &= 1+2(k+1)\varepsilon\sqrt{1+(k+1)^2\varepsilon^2}+2(k+1)^2\varepsilon^2.\end{aligned}\tag{3.17}$$

In addition, the asymptotic approximation of the energy of the kth ($k\in\mathbb{N}$) excited state can be given as [9]

$$\begin{aligned}E_k &:= E_\varepsilon(\phi_k^\varepsilon)\approx E_k^{\rm MA}\\ &= \frac{1}{2}+\frac{4}{3}(k+1)\varepsilon\sqrt{1+(k+1)^2\varepsilon^2}+2(k+1)^2\varepsilon^2.\end{aligned}\tag{3.18}$$

Based on the above asymptotic results, we make the following observations for the eigenfunctions of the singularly perturbed nonlinear eigenvalue problem (2.2)-(2.3) under the constraint (2.4):

- Boundary layers are observed at $x=0$ and $x=1$ for ground and all excited states when $0<\varepsilon\ll 1$. The width of these layers is of $\mathcal{O}(\varepsilon)=\mathcal{O}(\beta^{-1/2})$ (see (2.1)).
- For the kth ($k\in\mathbb{N}$) excited state, interior layers are also observed at $x_j=\frac{j}{k+1}$ ($j=1,2,\cdots,k$) when $0<\varepsilon\ll 1$. The widths of these layers are also of $\mathcal{O}(\varepsilon)=\mathcal{O}(\beta^{-1/2})$ (see (2.1)) and they are twice the size of the widths of the boundary layers.
- When $0<\varepsilon\ll 1$, if we rank all different eigenfunctions monotonously according to their energies, then the corresponding eigenvalues (or chemical potentials) are in the same order (see (3.14), (3.15), (3.17) and (3.18)).

These information will be used in designing the uniformly convergent numerical method for (2.2)-(2.4) in the next section.

3.2 For the whole space $\Omega=\mathbb{R}^d$ with harmonic potential

Again for simplicity, here we only present results for $d=1$ and $\Omega=\mathbb{R}$ with the harmonic potential, i.e., $V(x)=x^2/2$. Extensions to d-dimensions are straightforward. In this case, when $0<\varepsilon\ll 1$, we formally drop the first term on the right hand side of (2.11) with $d=1$ and obtain

$$\mu^{\rm TF}\phi^{\rm TF}(x)=\frac{x^2}{2}\phi^{\rm TF}(x)+|\phi^{\rm TF}(x)|^2\phi^{\rm TF}(x),\qquad x\in\mathbb{R},\tag{3.19}$$

which immediately implies that the Thomas-Fermi approximation for the ground state is

$$\phi_g^{\rm TF}(x)=\begin{cases}\sqrt{\mu_g^{\rm TF}-\frac{x^2}{2}}, & x^2<2\mu_g^{\rm TF},\\ 0, & \text{otherwise.}\end{cases}\tag{3.20}$$

Thus there is no boundary or interior layer in the ground state of BEC with harmonic potential. Plugging (3.20) into the constraint (2.12) with $d=1$, we get

$$1=\int_{-\infty}^{\infty}|\phi_g^{\rm TF}(x)|^2\,dx=\int_{-\sqrt{2\mu_g^{\rm TF}}}^{\sqrt{2\mu_g^{\rm TF}}}\left(\mu_g^{\rm TF}-\frac{x^2}{2}\right)dx=\frac{2}{3}\left(2\mu_g^{\rm TF}\right)^{3/2}. \tag{3.21}$$

Solving the above equation, we can obtain the asymptotic approximation for the eigenvalue (or chemical potential) of the ground state as

$$\mu_g^\varepsilon=\mu_\varepsilon(\phi_g^\varepsilon)\approx\mu_g^{\rm TF}=\frac{1}{2}\left(\frac{3}{2}\right)^{2/3}. \tag{3.22}$$

Furthermore, we can also obtain the asymptotic approximation for the energy of the ground state as

$$\begin{aligned}E_g^\varepsilon &= E_\varepsilon(\phi_g^\varepsilon)=\mu_\varepsilon(\phi_g^\varepsilon)-\frac{1}{2}\int_{-\infty}^{\infty}|\phi_g^\varepsilon(x)|^4\,dx\\ &\approx \mu_g^{\rm TF}-\frac{1}{2}\int_{-\infty}^{\infty}|\phi_g^{\rm TF}(x)|^4\,dx=\mu_g^{\rm TF}-\frac{2}{5}\mu_g^{\rm TF}=\frac{3}{10}\left(\frac{3}{2}\right)^{2/3}.\end{aligned} \tag{3.23}$$

In addition, the Thomas-Fermi approximation for the first excited state is

$$\phi_1^{\rm TF}(x)=\begin{cases}\sqrt{\mu_1^{\rm TF}-\frac{x^2}{2}}, & 0<x\le\sqrt{2\mu_1^{\rm TF}},\\ -\sqrt{\mu_1^{\rm TF}-\frac{x^2}{2}}, & -\sqrt{2\mu_1^{\rm TF}}\le x<0,\\ 0, & \text{otherwise.}\end{cases} \tag{3.24}$$

Similarly, we can get the Thomas-Fermi approximation for the eigenvalue (or chemical potential) and energy of the first excited state as

$$\mu_1^\varepsilon=\mu_\varepsilon(\phi_1^\varepsilon)\approx\mu_1^{\rm TF}=\frac{1}{2}\left(\frac{3}{2}\right)^{2/3},\qquad E_1^\varepsilon=E_\varepsilon(\phi_1^\varepsilon)=E_1^{\rm TF}\approx\frac{3}{10}\left(\frac{3}{2}\right)^{2/3}. \tag{3.25}$$

Since $\mu_1^{\rm TF}>0$ is independent of ε, when $0<\varepsilon\ll 1$, there is an interior layer located at $x=0$ in the first excited state of BEC with harmonic potential.

To get the matched asymptotic approximation for the first excited state, let us assume that the interior layer is of width δ with $0<\delta\ll 1$ and do a rescaling in the region near $x=0$ with

$$x=\delta X,\qquad \phi^\varepsilon(x)=\phi_s\,\Phi(X),\qquad X\ge 0. \tag{3.26}$$

Substituting (3.26) into (2.11) with $d=1$, we obtain

$$\mu^\varepsilon\,\Phi(X)=-\frac{\varepsilon^2}{2\delta^2}\,\Phi_{XX}(X)+\frac{\delta^2X^2}{2}\Phi(\delta X)+\phi_s^2\,\Phi^3(X),\qquad X>0, \tag{3.27}$$

$$\Phi(0)=0,\qquad \lim_{X\to\infty}\Phi(X)=1. \tag{3.28}$$

Since δ is small and we want to find approximate solution of (3.27) for $|X|$ not too large, we drop the second term in the right hand side of (3.27) and choose δ and ϕ_s as those in (3.8), we can obtain that (3.9) is an approximate solution of (3.27) for $|X|$ not too large. Since $\mu^\varepsilon \approx \mu_1^{\rm TF} = \mathcal{O}(1)$ for the first excited state, we can conclude that the width of the interior at $x=0$ is $\delta = \mathcal{O}(\varepsilon)$ and the inner expansion of (2.11) with $d=1$ near $x=0$ is

$$\phi_1^\varepsilon(x) = \sqrt{\mu_1^\varepsilon}\tanh\left(\sqrt{\mu_1^\varepsilon}x/\varepsilon\right), \qquad \text{for} \quad x\to 0. \tag{3.29}$$

Again, by using the matched asymptotic technique, we get the asymptotic approximation for the first excited state as

$$\begin{aligned}
&\phi_1^\varepsilon(x) \approx \phi_1^{\rm MA}(x)\\
&= \begin{cases}
\sqrt{\mu_1^{\rm MA}}\tanh\left(\sqrt{\mu_1^{\rm MA}}x/\varepsilon\right) + \sqrt{\mu_1^{\rm MA}-\frac{x^2}{2}} - \sqrt{\mu_1^{\rm MA}}, & 0\le x\le \sqrt{2\mu_1^{\rm TF}},\\
\sqrt{\mu_1^{\rm MA}}\tanh\left(\sqrt{\mu_1^{\rm MA}}x/\varepsilon\right) - \sqrt{\mu_1^{\rm MA}-\frac{x^2}{2}} + \sqrt{\mu_1^{\rm MA}}, & -\sqrt{2\mu_1^{\rm TF}}\le x<0,\\
0, & \text{otherwise;}
\end{cases}\\
&= \begin{cases}
\sqrt{\mu_1^{\rm MA}}\tanh\left(\sqrt{\mu_1^{\rm MA}}x/\varepsilon\right) - \dfrac{|x|x}{2\left[\sqrt{\mu_1^{\rm MA}-x^2/2}+\sqrt{\mu_1^{\rm MA}}\right]}, & x^2\le 2\mu_1^{\rm MA},\\
0, & \text{otherwise,}
\end{cases}
\end{aligned} \tag{3.30}$$

where $\mu_1^{\rm MA} = \mu_1^{\rm TF} + \mathcal{O}(\varepsilon)$ can be determined from the normalization constraint (2.12) with $d=1$ and $\phi = \phi_1^{\rm MA}$.

Based on the above asymptotic results, we make the following observations for the eigenfunctions of the singularly perturbed nonlinear eigenvalue problem (2.11) under the constraint (2.12):

- For the ground state, there is no boundary and interior layer.
- For the first excited state, an interior layer is located at $x=0$ and its width is of $\mathcal{O}(\varepsilon) = \mathcal{O}(\beta^{-1/3})$ (see (2.10)).

Again, these information will be used in designing the uniformly convergent numerical method for (2.11)-(2.12) in the next section.

4 A uniformly convergent numerical method

In this section, we will present a uniformly convergent numerical method for computing the eigenfunctions, i.e. ground and excited states, of the singularly perturbed nonlinear eigenvalue problem (2.18)-(2.20) under a constraint.

4.1 The normalized gradient flow

Various algorithms for computing the eigenfunctions, such as the ground and first excited states, of the nonlinear eigenvalue problem (2.18) under the constraint (2.20) have been studied in the literature. For instance, a Gauss-Seidel iterative method was proposed in [17] and a Lypuoniv functional method was presented in [15]. Perhaps one of the more popular and efficient techniques for dealing the constraint (2.20) is through the following construction: Choose a time step $k=\Delta t>0$ and denote a time sequence $0=t_0<t_1<\cdots<t_n<\cdots$ with $t_n=n\,k=n\,\Delta t$. To compute the ground and first excited states of the singularly perturbed nonlinear eigenvalue problem (2.18)-(2.19) under the constraint (2.20), it is natural to consider the following normalized gradient flow (NGF) which was widely used in the literature for computing the ground state solution of BEC [2,4,5]:

$$\partial_t\phi^\varepsilon(\mathbf{x},t)=-\frac{1}{2}\frac{\delta E_\varepsilon(\phi^\varepsilon)}{\delta\phi^\varepsilon}=\frac{\varepsilon^2}{2}\nabla^2\phi^\varepsilon-V(\mathbf{x})\phi^\varepsilon-|\phi^\varepsilon|^2\phi^\varepsilon,\ \mathbf{x}\in\Omega,\ t_n\le t<t_{n+1}, \tag{4.1}$$

$$\phi^\varepsilon(\mathbf{x},t_{n+1}):=\phi^\varepsilon(\mathbf{x},t_{n+1}^+)=\frac{\phi^\varepsilon(\mathbf{x},t_{n+1}^-)}{\|\phi^\varepsilon(\mathbf{x},t_{n+1}^-)\|},\qquad \mathbf{x}\in\Omega,\quad n\ge 0, \tag{4.2}$$

$$\phi^\varepsilon(\mathbf{x},t)=0,\qquad \mathbf{x}\in\Gamma=\partial\Omega,\qquad\qquad \phi^\varepsilon(\mathbf{x},0)=\phi_0^\varepsilon(\mathbf{x}),\qquad \mathbf{x}\in\Omega; \tag{4.3}$$

where

$$\phi^\varepsilon(\mathbf{x},t_n^\pm)=\lim_{t\to t_n^\pm}\phi^\varepsilon(\mathbf{x},t),\quad \|\phi_0^\varepsilon\|^2=\int_\Omega|\phi_0^\varepsilon(\mathbf{x})|^2\,d\mathbf{x}=1.$$

4.2 Discretization

Various spatial/temporal discretization schemes were studied and compared in the literature for discretizing the gradient flow (4.1)-(4.3) with uniform spatial meshes [2,4–6,11,12]. Here we adapt the backward Euler finite difference discretization scheme for (4.1)-(4.3) with a general spatial mesh. For simplicity of notation, we introduce the method for the case of one spatial dimension, i.e., $d=1$ in (4.1)-(4.3) with $\Omega=(a,b)$. Generalizations to higher dimensions are straightforward for tensor product grids. Let $a=x_0<x_1<\cdots<x_N=b$ be a partition of the interval $\Omega=(a,b)$, $h_j:=\Delta x_j=x_{j+1}-x_j$ be the length of the j-th ($j=0,1,\cdots,N-1$) subinterval, and $h=\max_{0\le j\le N-1}h_j$ be the mesh size of the partition. Denote ϕ_j^n be the approximation of $\phi^\varepsilon(x_j,t_n)$ and $\Phi^n=(\phi_0^n,\phi_1^n,\cdots,\phi_N^n)^T$ to be the solution vector at time $t=t_n$. The gradient flow (4.1) is discretized in time by the backward Euler scheme and in space by the finite difference method, for $j=1,\cdots,N-1$ and $n\ge 0$, as

$$\frac{\phi_j^*-\phi_j^n}{\Delta t}=\frac{\varepsilon^2}{2}\left[\frac{2\phi_{j-1}^*}{h_{j-1}(h_{j-1}+h_j)}-\frac{2\phi_j^*}{h_{j-1}h_j}+\frac{2\phi_{j+1}^*}{h_j(h_{j-1}+h_j)}\right]-V(x_j)\phi_j^*-|\phi_j^n|^2\phi_j^*. \tag{4.4}$$

The boundary and initial conditions (4.3) are discretized as

$$\phi_0^*=\phi_N^*=0,\qquad \phi_j^0=\phi_0^\varepsilon(x_j),\qquad j=0,1,\cdots,N. \tag{4.5}$$

The normalized step (4.2) is discretized as

$$\phi_j^{n+1}=\frac{\phi_j^*}{\|\Phi^*\|},\qquad j=0,1,\cdots,N,\qquad n\geq 0, \tag{4.6}$$

with

$$\begin{aligned}\|\Phi^*\| &= \sum_{j=1}^{N-1}\frac{h_{j-1}+h_j}{2}\left|\phi_j^*\right|^2=\sum_{j=0}^{N-1}\frac{h_j}{2}\left[\left|\phi_j^*\right|^2+\left|\phi_{j+1}^*\right|^2\right]\\ &\approx \sum_{j=0}^{N-1}\int_{x_j}^{x_{j-1}}|\phi^*(x)|^2\,dx=\int_a^b|\phi^*(x)|^2\,dx.\end{aligned} \tag{4.7}$$

In addition, the chemical potential (2.21) can be discretized as

$$\begin{aligned}\mu^\varepsilon &:= \frac{\varepsilon^2}{2}\int_a^b\left|\frac{d\phi^\varepsilon(x)}{dx}\right|^2dx+\int_a^b\left[V(x)|\phi^\varepsilon(x)|^2+|\phi^\varepsilon(x)|^4\right]d\mathbf{x}\\ &= \frac{\varepsilon^2}{2}\sum_{j=0}^{N-1}\int_{x_j}^{x_{j+1}}\left|\frac{d\phi^\varepsilon(x)}{dx}\right|^2dx+\sum_{j=0}^{N-1}\int_{x_j}^{x_{j+1}}\left[V(x)|\phi^\varepsilon(x)|^2+|\phi^\varepsilon(x)|^4\right]d\mathbf{x}\\ &\approx \frac{\varepsilon^2}{2}\sum_{j=0}^{N-1}h_j\left|\frac{\phi_{j+1}^\varepsilon-\phi_j^\varepsilon}{h_j}\right|^2+\sum_{j=0}^{N-1}\frac{h_j}{2}\sum_{l=j}^{j+1}\left[V(x_l)|\phi_l^\varepsilon|^2+|\phi_l^\varepsilon|^4\right]\\ &= \frac{\varepsilon^2}{2}\sum_{j=0}^{N-1}\frac{\left|\phi_{j+1}^\varepsilon-\phi_j^\varepsilon\right|^2}{h_j}+\sum_{j=1}^{N-1}\frac{h_j+h_{j-1}}{2}\left[V(x_j)|\phi_j^\varepsilon|^2+|\phi_j^\varepsilon|^4\right].\end{aligned} \tag{4.8}$$

Similarly, the energy functional (2.22) is discretized as

$$E_\varepsilon(\phi^\varepsilon)\approx\frac{\varepsilon^2}{2}\sum_{j=0}^{N-1}\frac{\left|\phi_{j+1}^\varepsilon-\phi_j^\varepsilon\right|^2}{h_j}+\sum_{j=1}^{N-1}\frac{h_j+h_{j-1}}{2}\left[V(x_j)|\phi_j^\varepsilon|^2+\frac{1}{2}|\phi_j^\varepsilon|^4\right]. \tag{4.9}$$

4.3 Choice of the piecewise uniform mesh

Based on the asymptotic results in the previous section, since we know the locations and width of the boundary and interior layers, the natural and simple way is to use the piecewise uniform mesh or Shishkin mesh [22, 23, 25, 29–32] in order to get a uniformly converged numerical method for $\varepsilon>0$.

In the case of box potential, we take $\Omega=(0,1)$, i.e., $a=0$ and $b=1$. For computing the ground state, since there are two boundary layers located at $x=0$ and $x=1$ with width $\mathcal{O}(\varepsilon)$, the piecewise uniform mesh can be chosen as

$$x_j=x_{j-1}+\begin{cases}h_1, & 0<j\leq N/4,\\ h_2, & N/4<j\leq 3N/4,\\ h_1, & 3N/4<j\leq N,\end{cases} \tag{4.10}$$

where

$$x_0=0,\qquad x_{N/4}=\min\{1/4,\,\varepsilon\ln N\},\qquad x_{3N/4}=1-x_{N/4},$$
$$x_N=1,\qquad h_1=\frac{4x_{N/4}}{N},\qquad h_2=\frac{2(x_{3N/4}-x_{N/4})}{N}.$$

In fact, here we use $N+1$ grid points in total for the interval $[0,1]$ with $N/4$ points for the boundary layer located at $x=0$, $N/4$ points for the boundary layer located at $x=1$, and $N/2$ points for the remaining middle portion. Similarly, for computing the first excited state, since there are two boundary layers located at $x=0$ and $x=1$ with width $\mathcal{O}(\varepsilon)$ and one interior layer located at $x=1/2$ with width $\mathcal{O}(2\varepsilon)$, the piecewise uniform mesh can be chosen as

$$x_j=x_{j-1}+\begin{cases} h_1, & 0<j\le N/8,\\ h_2, & N/8<j\le 3N/8,\\ h_1, & 3N/8<j\le 5N/8,\\ h_2, & 5N/8<j\le 7N/8,\\ h_1, & 7N/8<j\le N,\end{cases} \tag{4.11}$$

where

$$x_0=0,\quad x_{N/8}=\min\left\{\frac{1}{8},\,\varepsilon\ln N\right\},\quad x_{3N/8}=\frac{1}{2}-x_{N/8},\quad x_{5N/8}=\frac{1}{2}+x_{N/8},$$
$$x_{7N/8}=1-x_{N/8},\qquad x_N=1,\qquad h_1=\frac{8x_{N/8}}{N},\qquad h_2=\frac{4(x_{3N/8}-x_{N/8})}{N}.$$

In fact, here we use $N+1$ grid points in total for the interval $[0,1]$ with $N/8$ points for the boundary layer located at $x=0$, $N/8$ points for the boundary layer located at $x=1$, $N/4$ points for the interior layer located at $x=1/2$, and $N/2$ points for the remaining two portions. By extending the above idea, we can construct the piecewise uniform meshes used for computing other excited states in the box potential in 1D. Extension to higher dimensions can be done similarly.

In the case of harmonic potential or any other potential satisfying

$$V(-x)=V(x),\qquad V(0)=0,\qquad \lim_{|x|\to\infty}V(x)=\infty,$$

we take $\Omega=(-c,c)$, i.e., $a=-c$ and $b=c$. For computing the ground state, since there is no boundary and interior layer, we can use the classical uniform mesh

$$x_j=-c+jh,\quad j=0,1,\cdots,N,\qquad h=2c/N. \tag{4.12}$$

For computing the first excited state, since there is an interior layer located at $x=0$ with width $O(\varepsilon)$, the piecewise uniform mesh can be chosen as

$$x_j=x_{j-1}+\begin{cases} h_2, & 0<j\le N/4,\\ h_1, & N/4<j\le 3N/4,\\ h_2, & 3N/4<j\le N,\end{cases} \tag{4.13}$$

where

$$x_0=-c<0,\quad x_N=c>0,\quad x_{3N/4}=\min\{c/2,\,\varepsilon\ln N\},\quad x_{N/4}=-x_{3N/4},$$
$$h_1=\frac{x_{3N/4}}{N},\qquad h_2=\frac{2(c-x_{3N/4})}{N}.$$

In fact, here we use $N+1$ grid points in total for the interval $[-c,c]$ with $N/2$ points for the interior layer located at $x=0$, and $N/2$ points for the remaining two portions. Extension to higher dimensions can be done similarly.

5 Numerical results

In this section, we first demonstrate that our discretization method with piecewise uniform mesh is uniformly convergent for $\varepsilon>0$ and also compare the results from the piecewise uniform mesh and uniform mesh. Then we apply the new method based on piecewise uniform mesh to compute the ground and excited states of BEC with box/harmonic /optical lattice potential in the semiclassical regime, i.e., $0<\varepsilon\ll 1$. In our computation, the stationary state is reached when

$$\max_{0\le j\le N}|\phi_j^{n+1}-\phi_j^n|<10^{-6}.$$

Table 1: Maximum errors, i.e., $\max_{0\le x\le 1}|\phi(x)-\phi^N(x)|$, for the ground state of BEC with box potential by using uniform mesh for different ε and grid points N.

N	2^4	2^6	2^8	2^{10}	2^{12}
$\varepsilon=0.1\times 2^{0}$	2.64E-2	1.70E-3	1.06E-4	6.58E-6	4.57E-7
$\varepsilon=0.1\times 2^{-2}$	3.92E-1	2.43E-2	1.41E-3	8.38E-5	5.08E-6
$\varepsilon=0.1\times 2^{-4}$	7.68E-1	3.82E-1	2.37E-2	1.36E-3	8.10E-5
$\varepsilon=0.1\times 2^{-6}$	9.24E-1	7.68E-1	3.79E-1	2.35E-2	1.35E-3
$\varepsilon=0.1\times 2^{-8}$	9.76E-1	9.24E-1	7.67E-1	3.79E-1	2.35E-2
$\varepsilon=0.1\times 2^{-10}$	9.93E-1	9.77E-1	9.24E-1	7.67E-1	3.78E-1
$\varepsilon=0.1\times 2^{-12}$	9.98E-1	9.93E-1	9.77E-1	9.24E-1	7.67E-1
$\varepsilon=0.1\times 2^{-14}$	9.99E-1	9.98E-1	9.93E-1	9.77E-1	9.24E-1
$\vdots$	$\vdots$	$\vdots$	$\vdots$	$\vdots$	$\vdots$
$\varepsilon\to 0$	9.99E-1	9.99E-1	9.99E-1	9.99E-1	9.99E-1

5.1 Comparison and convergence rate

Let $\phi(x)$ be the numerical 'exact' solution obtained by using piecewise uniform mesh with $N=2^{14}$ and $\phi^N(x)$ be the numerical solution with $N+1$ grid points. Tables 1 and 2 show the maximum errors, i.e., $\max_{0\le x\le 1}|\phi(x)-\phi^N(x)|$, for the ground state of box potential by using uniform mesh and piecewise uniform mesh (or Shishkin mesh), respectively, for different ε and grid points N; Tables 3 and 4 show similar results for the

Table 2: Maximum errors, i.e., $\max_{0\le x\le 1}|\phi(x)-\phi^N(x)|$, for the ground state of BEC with box potential by using piecewise uniform mesh for different ε and grid points N.

N	2^4	2^6	2^8	2^{10}	2^{12}
$\varepsilon=0.1\times 2^{0}$	2.64E-2	1.70E-3	1.06E-4	6.58E-6	4.57E-7
$\varepsilon=0.1\times 2^{-2}$	2.72E-2	4.01E-3	4.42E-4	4.32E-5	3.62E-6
$\varepsilon=0.1\times 2^{-4}$	2.70E-2	3.84E-3	4.27E-4	4.16E-5	3.68E-6
$\varepsilon=0.1\times 2^{-6}$	2.70E-2	3.81E-3	4.23E-4	4.12E-5	5.76E-6
$\varepsilon=0.1\times 2^{-8}$	2.69E-2	3.78E-3	4.22E-4	4.27E-5	5.71E-6
$\varepsilon=0.1\times 2^{-10}$	2.69E-2	3.78E-3	4.22E-4	4.27E-5	5.71E-6
$\varepsilon=0.1\times 2^{-12}$	2.70E-2	3.78E-3	4.22E-4	4.27E-5	5.71E-6
$\varepsilon=0.1\times 2^{-14}$	2.70E-2	3.78E-3	4.22E-4	4.27E-5	5.71E-6
$\vdots$	$\vdots$	$\vdots$	$\vdots$	$\vdots$	$\vdots$
$\varepsilon\to 0$	2.70E-2	3.78E-3	4.22E-4	4.27E-5	5.71E-6

Table 3: Maximum errors for the first excited state of BEC with box potential by using uniform mesh for different ε and grid points N.

N	2^4	2^6	2^8	2^{10}	2^{12}
$\varepsilon=0.1\times 2^{0}$	3.84E-2	2.51E-3	1.57E-4	9.87E-6	6.75E-7
$\varepsilon=0.1\times 2^{-2}$	4.05E-1	2.52E-2	1.52E-3	9.50E-5	5.61E-6
$\varepsilon=0.1\times 2^{-4}$	7.69E-1	3.85E-1	2.39E-2	1.38E-3	7.96E-5
$\varepsilon=0.1\times 2^{-6}$	9.23E-1	7.68E-1	3.80E-1	2.36E-2	1.35E-3
$\varepsilon=0.1\times 2^{-8}$	9.76E-1	9.24E-1	7.67E-1	3.79E-1	2.35E-2
$\varepsilon=0.1\times 2^{-10}$	9.93E-1	9.77E-1	9.24E-1	7.67E-1	3.78E-1
$\varepsilon=0.1\times 2^{-12}$	9.98E-1	9.93E-1	9.77E-1	9.24E-1	7.67E-1
$\varepsilon=0.1\times 2^{-14}$	9.99E-1	9.98E-1	9.93E-1	9.77E-1	9.24E-1
$\vdots$	$\vdots$	$\vdots$	$\vdots$	$\vdots$	$\vdots$
$\varepsilon\to 0$	9.99E-1	9.99E-1	9.99E-1	9.99E-1	9.99E-1

first excited state of box potential; and Tables 5 and 6 show the results for the first excited state of harmonic potential with $V(x)=x^2/2$. In addition, Tables 7, 8 and 9 compare the results for the ground state of box potential, for the first excited state of box potential, and for the first excited state of harmonic potential, respectively, by using uniform mesh and piecewise uniform mesh.

From Tables 1-9, we can draw the following conclusion: (i) For fixed $\varepsilon>0$, when the mesh size $h<\varepsilon$ and $h\to 0$, second order convergence rate is observed in both the uniform mesh and piecewise uniform mesh (c.f., Tables 1-6) ; (ii) for fixed mesh size $h>0$ with small value, when $\varepsilon\to 0$, the errors increase up to a fixed constant by using the uniform mesh due to the appearance of boundary and/or interior layers (c.f., Tables 1, 3 and 5), where the errors do not increase by using the piecewise uniform mesh (c.f., Tables 2, 4 and 6); (iii) when both $\varepsilon\to 0$ and the mesh size $h\to 0$ with keeping ε/h as a constant,

Table 4: Maximum errors for the first excited state of BEC with box potential by using piecewise uniform mesh for different ε and grid points N.

N	2^4	2^6	2^8	2^{10}	2^{12}
$\varepsilon=0.1\times 2^{0}$	3.84E-2	2.51E-3	1.57E-4	9.87E-6	6.75E-7
$\varepsilon=0.1\times 2^{-2}$	1.84E-1	1.86E-2	1.52E-3	9.50E-5	5.61E-6
$\varepsilon=0.1\times 2^{-4}$	1.66E-1	1.69E-2	1.66E-3	1.52E-4	1.40E-5
$\varepsilon=0.1\times 2^{-6}$	1.61E-1	1.66E-2	1.62E-3	1.50E-4	1.46E-5
$\varepsilon=0.1\times 2^{-8}$	1.60E-1	1.65E-2	1.62E-3	1.50E-4	1.45E-5
$\varepsilon=0.1\times 2^{-10}$	1.60E-1	1.65E-2	1.60E-3	1.49E-4	1.45E-5
$\varepsilon=0.1\times 2^{-12}$	1.60E-1	1.64E-2	1.63E-3	1.49E-4	1.45E-5
$\varepsilon=0.1\times 2^{-14}$	1.60E-1	1.64E-2	1.63E-3	1.49E-4	1.45E-5
$\vdots$	$\vdots$	$\vdots$	$\vdots$	$\vdots$	$\vdots$
$\varepsilon\to 0$	1.60E-1	1.64E-2	1.63E-3	1.49E-4	1.45E-5

Table 5: Maximum errors for the first excited state of BEC with harmonic potential $V(x)=x^2/2$ by using uniform mesh for different ε and grid points N.

N	2^4	2^6	2^8	2^{10}	2^{12}
$\varepsilon=0.1\times 2^{0}$	7.37E-1	5.89E-1	2.44E-1	1.24E-1	1.24E-1
$\varepsilon=0.1\times 2^{-2}$	7.87E-1	7.36E-1	5.88E-1	2.44E-1	1.57E-1
$\varepsilon=0.1\times 2^{-4}$	8.03E-1	7.87E-1	7.36E-1	5.89E-1	2.46E-1
$\varepsilon=0.1\times 2^{-6}$	8.07E-1	8.03E-1	7.87E-1	7.36E-1	5.90E-1
$\varepsilon=0.1\times 2^{-8}$	8.09E-1	8.07E-1	8.03E-1	7.87E-1	7.37E-1
$\varepsilon=0.1\times 2^{-10}$	8.09E-1	8.09E-1	8.07E-1	8.03E-1	7.87E-1
$\varepsilon=0.1\times 2^{-12}$	8.09E-1	8.09E-1	8.09E-1	8.07E-1	8.03E-1
$\varepsilon=0.1\times 2^{-14}$	8.09E-1	8.09E-1	8.09E-1	8.09E-1	8.07E-1
$\vdots$	$\vdots$	$\vdots$	$\vdots$	$\vdots$	$\vdots$
$\varepsilon\to 0$	8.09E-1	8.09E-1	8.09E-1	8.09E-1	8.09E-1

Table 6: Maximum errors for the first excited state of BEC with harmonic potential $V(x)=x^2/2$ by using piecewise uniform mesh for different ε and grid points N.

N	2^4	2^6	2^8	2^{10}	2^{12}
$\varepsilon=0.1\times 2^{0}$	2.26E-1	5.73E-2	3.97E-3	2.67E-4	1.76E-5
$\varepsilon=0.1\times 2^{-2}$	2.51E-1	9.30E-2	1.00E-2	1.02E-3	6.37E-5
$\varepsilon=0.1\times 2^{-4}$	2.61E-1	1.08E-1	1.84E-2	2.49E-3	2.57E-4
$\varepsilon=0.1\times 2^{-6}$	2.63E-1	1.11E-1	2.17E-2	3.49E-3	3.80E-4
$\varepsilon=0.1\times 2^{-8}$	2.63E-1	1.11E-1	2.19E-2	3.67E-3	3.59E-4
$\varepsilon=0.1\times 2^{-10}$	2.63E-1	1.12E-1	2.18E-2	3.69E-3	3.44E-4
$\varepsilon=0.1\times 2^{-12}$	2.63E-1	1.12E-1	2.18E-2	3.69E-3	3.40E-4
$\varepsilon=0.1\times 2^{-14}$	2.63E-1	1.12E-1	2.18E-2	3.69E-3	3.39E-4
$\vdots$	$\vdots$	$\vdots$	$\vdots$	$\vdots$	$\vdots$
$\varepsilon\to 0$	2.63E-1	1.12E-1	2.18E-2	3.69E-3	3.39E-4

no convergence is observed by using the uniform mesh, but uniformly convergent results are observed by using the piecewise uniform mesh (c.f., Tables 7, 8 and 9). Based on these results, we can claim that the backward Euler finite difference discretization by using the piecewise uniform mesh is a uniformly convergent numerical method for computing the singularly perturbed nonlinear eigenvalue problem (2.18)-(2.20) under a constraint.

Table 7: Comparison of the maximum errors for the ground state of BEC with box potential by using uniform mesh and piecewise uniform mesh.

N	2^4	2^6	2^8	2^{10}	2^{12}
ε	0.1×2^0	0.1×2^{-2}	0.1×2^{-4}	0.1×2^{-6}	0.1×2^{-8}
uniform mesh	2.64E-2	2.43E-2	2.37E-2	2.35E-2	2.35E-2
piecewise uniform mesh	2.64E-2	4.01E-3	4.27E-4	4.12E-5	5.71E-6

Table 8: Comparison of the maximum errors for the first state of BEC with box potential by using uniform mesh and piecewise uniform mesh.

N	2^4	2^6	2^8	2^{10}	2^{12}
ε	0.1×2^0	0.1×2^{-2}	0.1×2^{-4}	0.1×2^{-6}	0.1×2^{-8}
uniform mesh	3.84E-2	2.52E-2	2.39E-2	2.36E-2	2.35E-2
piecewise uniform mesh	3.84E-2	1.86E-2	1.66E-3	1.50E-4	1.45E-5

Table 9: Comparison of the maximum errors for the first excited state of BEC with harmonic potential $V(x)=x^2/2$ by using uniform mesh and piecewise uniform mesh.

N	2^4	2^6	2^8	2^{10}	2^{12}
ε	0.1×2^0	0.1×2^{-2}	0.1×2^{-4}	0.1×2^{-6}	0.1×2^{-8}
uniform mesh	7.37E-1	7.36E-1	7.36E-1	7.36E-1	7.37E-1
piecewise uniform mesh	2.26E-1	9.30E-2	1.84E-2	3.49E-3	3.59E-4

5.2 Applications

In this subsection, we report the ground and excited states of BEC with box, harmonic and optical lattice potential by using the backward Euler finite difference method based on the piecewise uniform mesh.

Example 5.1. Ground and excited states of BEC with box potential in 1D. Fig. 1 shows the ground and excited states of BEC with box potential in 1D for different ε and Table 10 lists their corresponding energy and chemical potential.

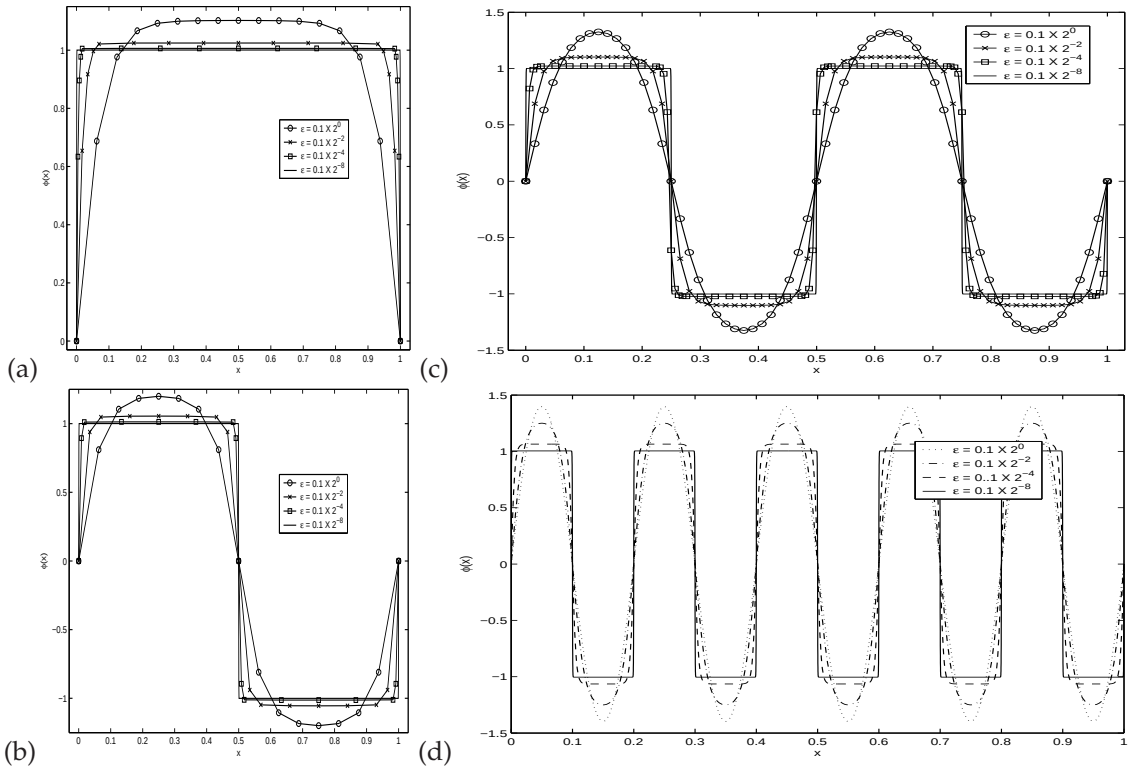

Figure 1: Ground and excited states of BEC with box potential in 1D for different ε. (a): Ground state with $N=2^4$; (b): first excited state with $N=2^4$; (c): third excited state with $N=2^6$; and (d): ninth excited state with $N=1280$.

Table 10: Energy and chemical potential of the ground and excited states of BEC with box potential in 1D for different ε.

ε	0.1×2^{-2}	0.1×2^{-4}	0.1×2^{-6}	0.1×2^{-8}
$E_g=E(\phi_g)$	0.5345	0.5084	0.5021	0.5005
$E_1=E(\phi_1)$	0.5718	0.5169	0.5042	0.5010
$E_3=E(\phi_3)$	0.6553	0.5345	0.5084	0.5021
$E_9=E(\phi_9)$	0.9938	0.5909	0.5210	0.5052
$\mu_g=\mu(\phi_g)$	1.0512	1.0126	1.0031	1.0008
$\mu_1=\mu(\phi_1)$	1.1051	1.0253	1.0063	1.0016
$\mu_3=\mu(\phi_3)$	1.2208	1.0511	1.0126	1.0031
$\mu_9=\mu(\phi_9)$	1.6400	1.1322	1.0314	1.0078

From Fig. 1 and Table 10 and additional results not shown here for brevity [14], we can draw the following conclusion for the ground and excited states of BEC with box potential in 1D: (i) Boundary layers are observed in ground and excited states and interior layers are observed in excited states when ε is small and the width of the boundary and

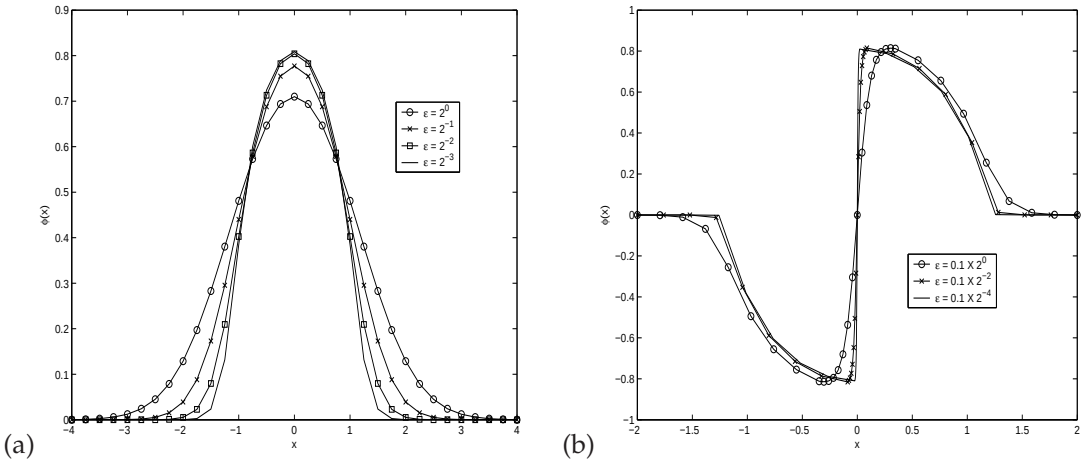

Figure 2: Ground and first excited states of BEC with harmonic potential in 1D for different ε. (a): Ground state with $N=2^5$ by using uniform mesh; (b): first excited state with $N=2^5$ by using piecewise uniform mesh.

Table 11: Energy and chemical potential of the ground and first excited states of BEC with harmonic potential in 1D for different ε.

ε	0.2	0.1	0.05	0.025	0.0125
$E_g=E(\phi_g)$	0.4164	0.4002	0.3952	0.3937	0.3933
$E_1=E(\phi_1)$	0.5787	0.4764	0.4320	0.4117	0.4022
$\mu_g=\mu(\phi_g)$	0.6676	0.6587	0.6561	0.6554	0.6552
$\mu_1=\mu(\phi_1)$	0.8180	0.7314	0.6920	0.6732	0.6641

interior layers is of $\mathcal{O}(\varepsilon)$ (c.f. Fig. 1), these confirm the asymptotic results in Section 3. (ii) For any fixed $\varepsilon>0$, if all different eigenfunctions of the nonlinear eigenvalue problem (2.18)-(2.20) under a constraint are ranked according to their energy, then the corresponding eigenvalues (or chemical potential) are in the same rank (c.f. Table 10), i.e.,

$$E(\phi_g)<E(\phi_1)<E(\phi_2)<\cdots \quad\Longrightarrow\quad \mu(\phi_g)<\mu(\phi_1)<\mu(\phi_2)<\cdots.$$

(iii) When $\varepsilon\to 0$, we have (c.f. Table 10)

$$\lim_{\varepsilon\to 0}E(\phi_g)=\lim_{\varepsilon\to 0}E(\phi_j)=\frac{1}{2},\qquad \lim_{\varepsilon\to 0}\mu(\phi_g)=\lim_{\varepsilon\to 0}\mu(\phi_j)=1,\quad j=1,2,\cdots,$$
$$\lim_{\varepsilon\to 0}\frac{E(\phi_g)}{\mu(\phi_g)}=\frac{1}{2},\qquad \lim_{\varepsilon\to 0}\frac{E(\phi_j)}{E(\phi_g)}=1,\qquad \lim_{\varepsilon\to 0}\frac{\mu(\phi_j)}{\mu(\phi_g)}=1,\quad j=1,2,\cdots.$$

Example 5.2. Ground and first excited states of BEC with harmonic potential in 1D. Fig. 2 shows the ground and first excited states of BEC with harmonic potential in 1D for different ε and Table 11 lists their corresponding energy and chemical potential.

From Fig. 2 and Table 11, we can draw the following conclusion for the ground and first excited states of BEC with harmonic potential in 1D: (i) Interior layer is observed

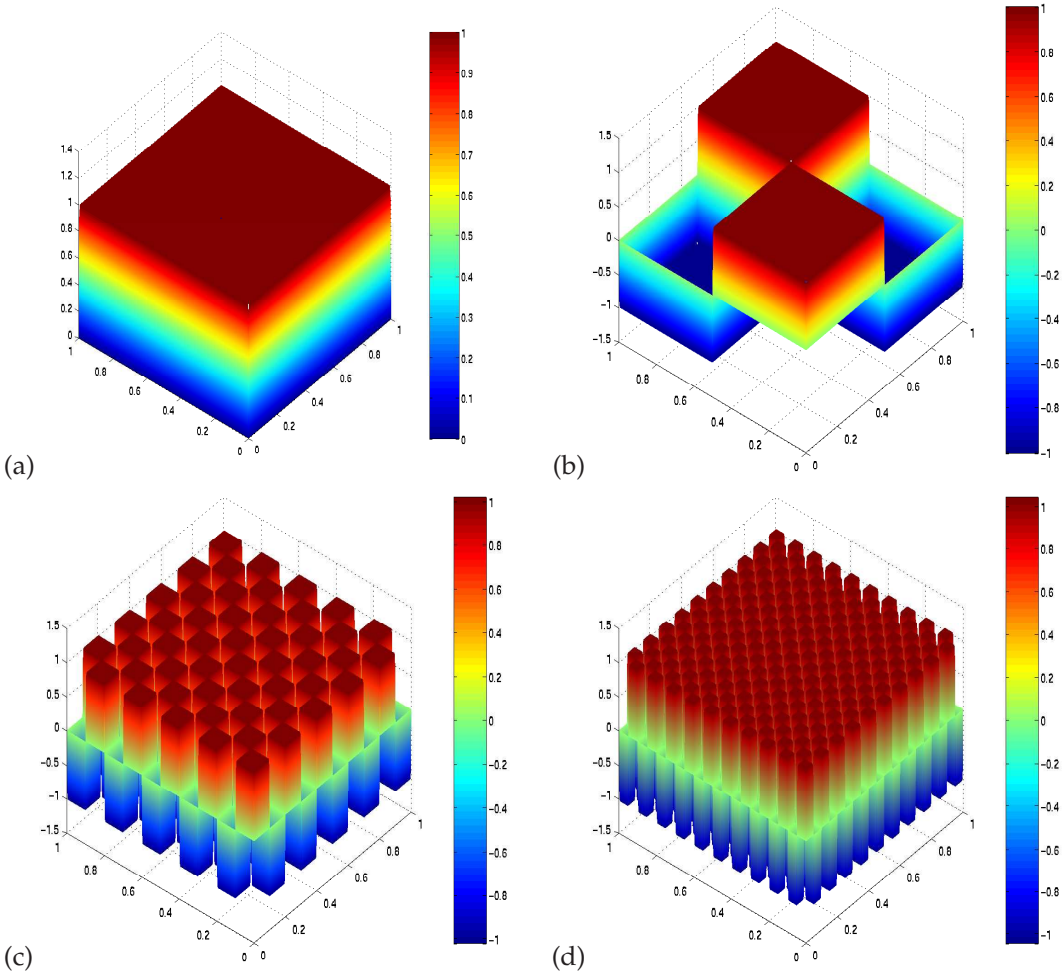

Figure 3: Surface plots for ground and excited states of BEC with box potential in 2D with $\varepsilon = 10^{-3}$. (a): Ground state; (b): (1,1)-th excited state; (c): (9,9)-th excited state; and (d) (19,19)-th excited state.

in the first excited state when ε is small and the width of the interior layer is of $O(\varepsilon)$ (c.f. Fig. 2), this confirms the asymptotic results in Section 3. (ii) For any fixed $\varepsilon > 0$, we have (c.f. Table 11)

$$E(\phi_g) < E(\phi_1) \quad \Longrightarrow \quad \mu(\phi_g) < \mu(\phi_1).$$

(iii) When $\varepsilon \to 0$, we have (c.f. Table 11)

$$\lim_{\varepsilon\to 0} E(\phi_g) = \lim_{\varepsilon\to 0} E(\phi_1) = \frac{3}{10}\left(\frac{3}{2}\right)^{2/3}, \qquad \lim_{\varepsilon\to 0} \mu(\phi_g) = \lim_{\varepsilon\to 0} \mu(\phi_1) = \frac{1}{2}\left(\frac{3}{2}\right)^{2/3},$$

$$\lim_{\varepsilon\to 0} \frac{E(\phi_g)}{\mu(\phi_g)} = \frac{3}{5}, \qquad \lim_{\varepsilon\to 0} \frac{E(\phi_1)}{E(\phi_g)} = 1, \qquad \lim_{\varepsilon\to 0} \frac{\mu(\phi_1)}{\mu(\phi_g)} = 1.$$

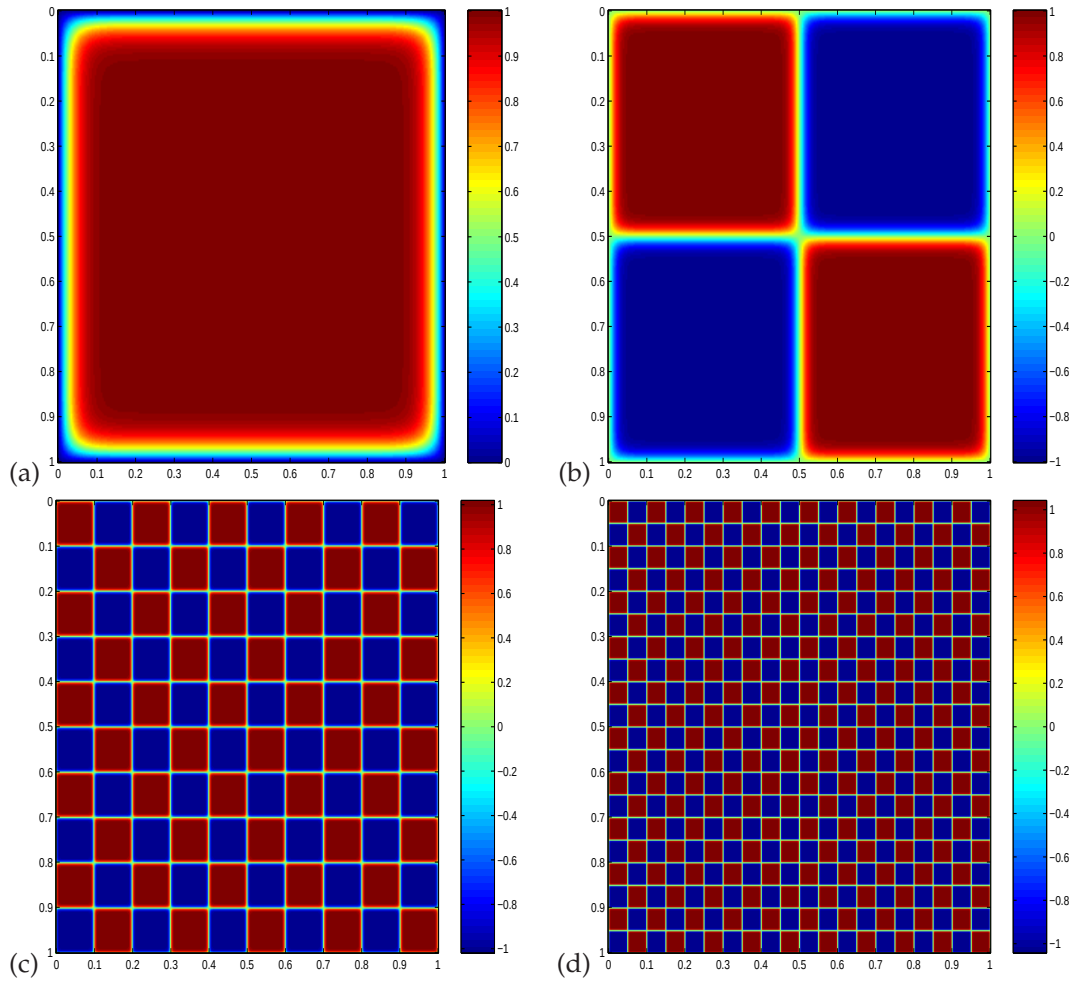

Figure 4: Contour plots for ground and excited states of BEC with box potential in 2D with $\varepsilon = 10^{-3}$. (a): Ground state; (b): (1,1)-th excited state; (c): (9,9)-th excited state; and (d) (19,19)-th excited state.

Example 5.3. Ground and excited states of BEC with box potential in 2D. Figs. 3 and 4 show surface plots and contour plots, respectively, for ground and excited states of BEC with box potential in 2D with $\varepsilon = 10^{-3}$ over a 257×257 piecewise uniform mesh.

From Figs. 3 and 4, similar conclusions as those for BEC with box potential in 1D can be drawn.

Example 5.4. Ground and first excited states of BEC with harmonic potential, i.e.,

$$V(x,y) = (x^2+y^2)/2,$$

in 2D. Figs. 5 and 6 show surface plots and contour plots, respectively, for ground and first excited states of BEC with harmonic potential in 2D with $\varepsilon = 1.56 \times 10^{-3}$ over a 257×257 piecewise uniform mesh.

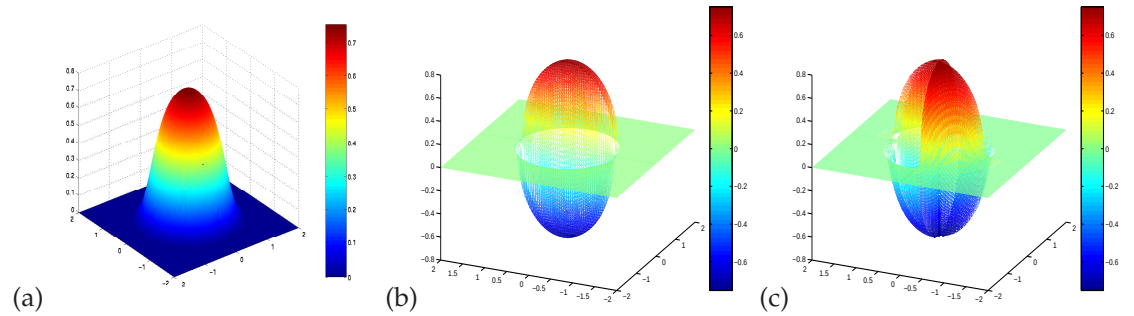

Figure 5: Surface plots for ground and first excited states of BEC with harmonic potential in 2D with $\varepsilon = 1.56\times10^{-3}$. (a): Ground state; (b): first excited state in x-direction; (c): first excited state in both x- and y-directions.

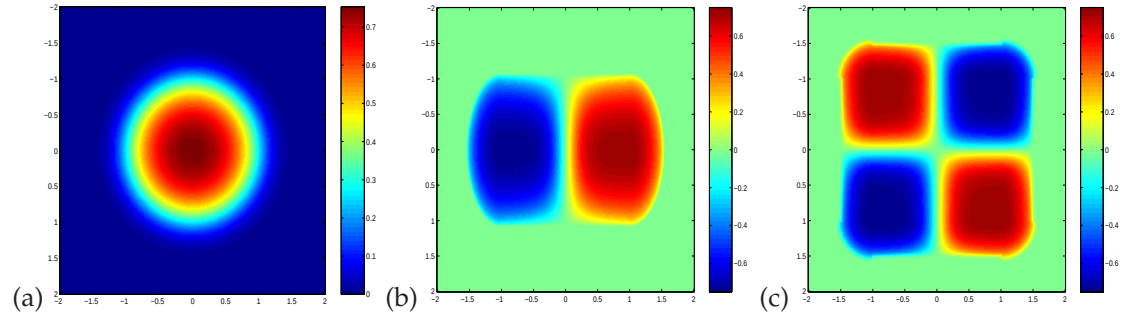

Figure 6: Contour plots for ground and first excited states of BEC with harmonic potential in 2D with $\varepsilon = 1.56\times10^{-3}$. (a): Ground state; (b): first excited state in x-direction; (c): first excited state in both x- and y-directions.

From Figs. 5 and 6, similar conclusions as those for BEC with harmonic potential in 1D can be drawn.

Example 5.5. Ground and asymmetric excited states of BEC with optical lattice potential, i.e.,

$$V(x,y) = (x^2+y^2)/2+0.3\sin^2(4\pi x)+0.3\sin^2(4\pi x),$$

in 2D. Figs. 7 and 8 show surface plots and contour plots, respectively, for ground and asymmetric excited states of BEC with optical lattice potential in 2D with $\varepsilon = 0.025$ over a 257×257 piecewise uniform mesh.

From Figs. 7 and 8, similar conclusions as those for BEC with harmonic potential in 2D can be drawn.

6 Conclusion

We have studied singularly perturbed nonlinear eigenvalue problems under constraints analytically and numerically. We began with the time-independent Gross-Pitaevskii equa-

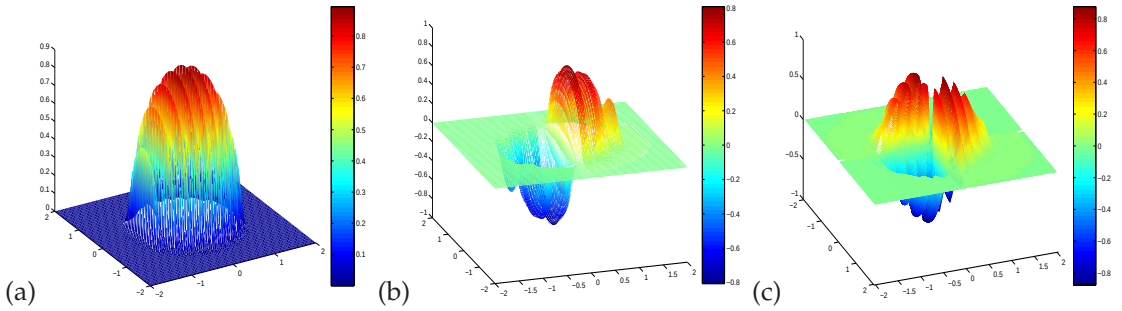

Figure 7: Surface plots for ground and asymmetric excited states of BEC with optical lattice potential in 2D with $\varepsilon = 0.025$. (a): Ground state; (b): asymmetric excited state in x-direction; (c): asymmetric excited state in both x- and y-directions.

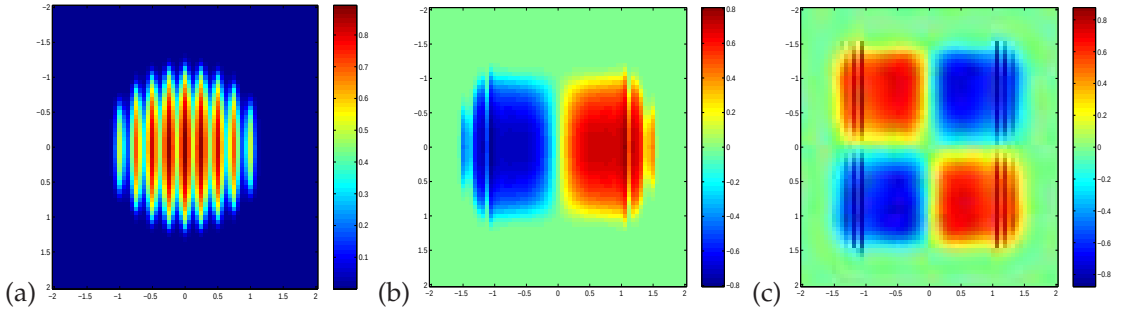

Figure 8: Contour plots for ground and asymmetric excited states of BEC with harmonic potential in 2D with $\varepsilon = 0.025$. (a): Ground state; (b): asymmetric excited state in x-direction; (c): asymmetric excited state in both x- and y-directions.

tion (GPE) for modelling Bose-Einstein condensates (BEC) and reformulated the GPE into singularly perturbed nonlinear eigenvalue problems under constraints. In the analytical side, we found matched asymptotic approximations for the ground and excited states for the problem under the box potential and the harmonic potential in the semiclassical regime, i.e., $0 < \varepsilon \ll 1$. These matched asymptotic approximations clearly indicated that boundary and interior layers appeared in the ground and excited states when ε is small. In addition, energy and eigenvalues (or chemical potential) asymptotics of the ground and excited states were also provided. In the numerical side, we proposed the backward Euler finite difference (BEFD) method based on piecewise uniform mesh or Shishkin mesh, which was demonstrated to be uniformly convergent for $\varepsilon > 0$, for computing the eigenfunctions of the nonlinear eigenvalue problems under a constraint. Numerical results showed that the new method gave much better results than those obtained from the BEFD based on standard uniform mesh in the semiclassical regime, i.e., $0 < \varepsilon \ll 1$. Finally, our method was applied to compute the ground and excited states of BEC with box, harmonic or optical lattice potential in one dimension (1D) and 2D. Some conclusive findings were reported and some conjectures were proposed based on our extensive numerical results.

Acknowledgments

The authors acknowledge support from Singapore Ministry of Education grant No. R-146-000-083-112 and would like to thank Professor Tao Tang for very helpful discussion on the subject.

References

[1] S. K. Adhikari, Numerical solution of the two-dimensional Gross-Pitaevskii equation for trapped interacting atoms, Phys. Lett. A, 265 (2000), 91.
[2] A. Aftalion and Q. Du, Vortices in a rotating Bose-Einstein condensate: Critical angular velocities and energy diagrams in the Thomas-Fermi regime, Phys. Rev. A, 64 (2001), 063603.
[3] M. H. Anderson, J. R. Ensher, M. R. Matthewa, C. E. Wieman and E. A. Cornell, Observation of Bose-Einstein condensation in a dilute atomic vapor, Science, 269 (1995), 198-201.
[4] W. Bao, Ground states and dynamics of multi-component Bose-Einstein condensates, Multiscale Modeling and Simulation, 2 (2004), 210-236.
[5] W. Bao and Q. Du, Computing the ground state solution of Bose-Einstein condensates by a normalized gradient flow, SIAM J. Sci. Comput., 25 (2004), 1674-1697.
[6] W. Bao, I.-L. Chern and F. Y. Lim, Efficient and spectrally accurate numerical methods for computing ground and first excited states in Bose-Einstein condensates, J. Comput. Phys., 219 (2006), 836-854.
[7] W. Bao, D. Jaksch and P. A. Markowich, Numerical solution of the Gross-Pitaevskii equation for Bose-Einstein condensation, J. Comput. Phys., 187 (2003), 318-342.
[8] W. Bao and F. Y. Lim, Computing ground states of spin-1 Bose-Einstein Condensates by the normalized gradient flow, SIAM J. Sci. Comput., in press.
[9] W. Bao, F. Y. Lim and Y. Zhang, Energy and chemical potential asymptotics for the ground state of Bose-Einstein condensates in the semiclassical regime, Bull. Inst. Math., Academia Sinica, 2 (2007), 495-532.
[10] W. Bao and W. Tang, Ground state solution of trapped interacting Bose-Einstein condensate by directly minimizing the energy functional, J. Comput. Phys., 187 (2003), 230-254.
[11] W. Bao and H. Wang, A mass and magnetization conservative and energy diminishing numerical method for computing ground state of spin-1 Bose-Einstein condensates, SIAM J. Numer. Anal., 45 (2007), 2177-2200.
[12] W. Bao, H. Wang and P. A. Markowich, Ground, symmetric and central vortex states in rotating Bose-Einstein condensates, Commun. Math. Sci., 3 (2005), 57-88.
[13] M. M. Cerimele, M. L. Chiofalo, F. Pistella, S. Succi and M. P. Tosi, Numerical solution of the Gross-Pitaevskii equation using an explicit finite-difference scheme: An application to trapped Bose-Einstein condensates, Phys. Rev. E, 62, 1382 (2000).
[14] M. H. Chai, A Uniformly Convergent Numerical Method Scheme for Singularly Perturbed Nonlinear Eigenvalue Problems Under Constraints, MSc Thesis, Department of Mathematics, National University of Singapore, 2007.
[15] S.-L. Chang, C.-S. Chien and B.W. Jeng, Liapunov-Schmidt reduction and continuation for nonlinear Schrödinger equations, SIAM J. Sci. Comput., 27 (2007), 729-755.
[16] S.-M. Chang, W.-W. Lin and S.-F. Shieh, Gauss-Seidel-type methods for energy states of a multi-component Bose-Einstein condensate, J. Comput. Phys., 202 (2005), 367-390.

[17] S.-M. Chang, C. S. Lin, T. C. Lin and W. W. Lin, Segregated nodal domains of two-dimensional multispecies Bose-Einstein condensates, Physica D, 196 (2004), 341-361.
[18] M. L. Chiofalo, S. Succi and M. P. Tosi, Ground state of trapped interacting Bose-Einstein condensates by an explicit imaginary-time algorithm, Phys. Rev. E, 62 (2000), 7438.
[19] F. Dalfovo and S. Stringari, Bosons in anisotropic traps: Ground state and vortices, Phys. Rev. A, 53 (1996), 2477.
[20] R. J. Dodd, Approximate solutions of the nonlinear Schrödinger equation for ground and excited states of Bose-Einstein condensates, J. Res. Natl. Inst. Stan., 101 (1996), 545.
[21] M. Edwards and K. Burnett, Numerical solution of the nonlinear Schrödinger equation for small samples of trapped neutral atoms, Phys. Rev. A, 51 (1995), 1382.
[22] J. J. H. Miller, E. O'Riordan and G. I. Shishkin, Fitted Numerical Mehtods for Sigular Perturbation Problems, World Scientific, 1996.
[23] J. J. H. Miller, E. O'Riordan and G. I. Shishkin, On piecewise-uniform meshes for upwind- and central-difference operators for solving singularly perturbed problems, IMA J. Numer. Anal., 15 (1995), 89-99.
[24] L. P. Pitaevskii and S. Stringari, Bose-Einstein Condensation, Clarendon Press, 2003.
[25] H. G. Roos, M. Stynes and L. Tobiska, Numerical Methods for Singularly Perturbed Differential Equations, Springer-Verlag, Berlin, 1996.
[26] P. A. Ruprecht, M. J. Holland, K. Burrett and M. Edwards, Time-dependent solution of the nonlinear Schrodinger equation for Bose-condensed trapped neutral atoms, Phys. Rev. A, 51 (1995), 4704-4711.
[27] B. I. Schneider and D. L. Feder, Numerical approach to the ground and excited states of a Bose-Einstein condensated gas confined in a completely anisotropic trap, Phys. Rev. A, 59 (1999), 2232.
[28] L. H. Shen and A. H. Zhou, A defect correction scheme for finite element eigenvalues with applications to quantum chemistry, SIAM J. Sci. Comput., 28 (2006), 321-338.
[29] G. I. Shishkin, Grid approximation of singularly perturbed elliptic and parabolic equations, Second Doctoral Thesis, Keldysh Institute of Applied Mathematics, USSR Academy of Sciences, Moscow, 1990.
[30] T. Tang and M. R. Trummer, Boundary layer resolving pseudospectral methods for singular perturbation problems, SIAM J. Sci. Comput., 17 (1996), 430-438.
[31] Y. Qiu, D. M. Sloan and T. Tang, Numerical solution of a singularly perturbed two-point boundary value problem using equidistribution: analysis of convergence, J. Comput. Appl. Math., 116 (2000), 121-143.
[32] A. B. White, On Selection of equidistribution meshes for two-point boundary value problems, SIAM J. Numer. Anal., 16 (1979), 472-502.
[33] A. H. Zhou, Finite dimensional approximations for the electronic ground state solution of a molecular system, Math. Methods Appl. Sci., 30 (2007), 429-447.
[34] A. H. Zhou, An analysis of finite-dimensional approximations for the ground state solution of Bose-Einstein condensates, Nonlinearity 17 (2004), 541-550.